Numerical Model of Sediment Pulses and Sediment-Supply Disturbances in Mountain Rivers

Yantao Cui, M.ASCE,[1] and Gary Parker, M.ASCE[2]

Abstract: Sediment pulses in rivers can result from many mechanisms including landslides entering from side slopes and debris flows entering from tributaries. Artificial sediment pulses can be caused by the removal of a dam. This paper presents a numerical model for the simulation of gravel bedload transport and sediment pulse evolution in mountain rivers. A combination of the backwater and quasi-normal flow formulations is used to calculate flow parameters. Gravel bedload transport is calculated with the surface-based bedload equation of Parker in 1990. The Exner equation of sediment continuity is used to express the mass balance at different grain size groups and lithologies, as well as the abrasion of gravel. The river is assumed to have no geological controls such as bedrock outcrops and immobile boulder pavements. The results of nine numerical experiments designed to study various key parameters relevant to the evolution of sediment pulses are reported here. Results of the numerical runs indicate that the evolution of sediment pulses in mountain rivers is dominated by dispersion rather than translation. Here dispersion is an expression for the observation that a sediment pulse aggrades both upstream and downstream of its apex whereas its amplitude decreases in time. The results also indicate that grain abrasion is an important and yet often neglected mechanism in removing the excess sediment associated with pulse inputs from some mountain rivers.

DOI: 10.1061/(ASCE)0733-9429(2005)131:8(646)

CE Database subject headings: Sediment transport; Numerical models; Channel morphology; Mountain streams; Movable bed models.

Introduction

Large-scale sediment pulses (or waves) in rivers are known to occur naturally, in response to, for example, landslides or debris flows from tributaries, which may in turn be associated with hydrologic events such as an extreme flood following a long period of drought. Human activities such as mining, forest harvesting, and road construction can increase the magnitude and frequency of these events. A classic documentation of sediment pulses pertains to rivers flowing off the western slopes of the Sierra Nevada, California (Gilbert 1917; James 1991). In this case massive amounts of mining waste dumped into the rivers propagated downstream and caused as much as several meters of aggradation. After mining ceased in 1884, the rivers underwent subsequent degradation. To date, the rivers have not yet recovered to their premining grades. Pickup et al. (1983) and Knighton (1989) have documented similar problems associated with mining in the Kawerong River, Papua New Guinea and the Ringarooma River, Tasmania, respectively. In both cases the pulse of aggradation due to mining waste disposal traveled slowly in the downstream direction and became longer and flatter as it propagated.

Sediment pulses due to natural events have also been documented. For example, a landslide occurred in March 1995 on the Navarro River near Floodgate, California, delivering approximately 60,000–80,000 m^3 of material into the channel, blocking the river for several hours and creating a pond that extended over 1.5 km upstream through the fall of 1995 (Hansler 1999; Lisle et al. 2001; Sutherland et al. 2002). Detailed surveys in 1996 and 1997 have indicated that the sediment pulse was predominantly dispersing in place with little downstream translation (Hansler 1999; Sutherland et al. 2002).

The past research on the evolution of sediment pulses to date has been focused on field observations, laboratory experiments, numerical models, and simplified analytical solutions (e.g., Gilbert 1917; Weir 1983; James 1991; Pickup et al. 1983; Knighton 1989; Lisle et al. 1997, 2001; Benda and Dunne 1997; Sutherland et al. 2002; Cui et al. 2003a,b). One of the most recent physically based numerical models is that of Lisle et al. (1997), which helped inspire the present work, including that presented in Cui et al. (2003a,b). The model presented in this paper expends upon the model of Lisle et al. (1997) in three aspects: (1) to consider the transport and conservation of heterogeneous sediment; (2) to consider particle abrasion of different lithologies in a sediment mixture; and (3) to consider transient flow in solution techniques. Six runs were conducted to test the relative importance of the major parameters that are relevant to the evolution of sediment pulses. In addition, two more runs were conducted to explore the effect of varied supply of the material that constitutes the initial sediment pulse. It should be noted that the purpose of the runs is to provide a qualitative examination of the relative importance of the parameters tested so that they can be given proper attention in future

[1]Hydraulic Engineer, Stillwater Sciences, 2855 Telegraph Ave., Berkeley, CA 94705; formerly, Research Associate, St. Anthony Falls Laboratory, Univ. of Minnesota, Minneapolis, MN 55414. E-mail: yantao@stillwatersci.com

[2]Professor, St. Anthony Falls Laboratory, Univ. of Minnesota, Mississippi River at Third Ave. S.E., Minneapolis, MN 55414. E-mail: parke002@umn.edu

Note. Discussion open until January 1, 2006. Separate discussions must be submitted for individual papers. To extend the closing date by one month, a written request must be filed with the ASCE Managing Editor. The manuscript for this paper was submitted for review and possible publication on November 4, 2002; approved on December 30, 2004. This paper is part of the ***Journal of Hydraulic Engineering***, Vol. 131, No. 8, August 1, 2005. ©ASCE, ISSN 0733-9429/2005/8-646–656/$25.00.

research, model development and engineering projects.

The model presented in this paper provided the foundation for several derivatives that were written to simulate specific engineering and research problems such as the removal of a dam and the simulation of laboratory experiments [e.g., Cui and Wilcox (2005) and Cui et al. (2005a, 2003b)]. Neither of these documents, however, provides a comprehensive exposition of model formulation, a task that is accomplished in the present paper. Exposition of the basic model of this paper serves to outline the basic theories and hypothesis underlying those derivative models. In addition to the derivatives of the models, Hansler (1999), Lisle et al. (2001), and Sutherland et al. (2002) also applied the present model to simulate the evolution of a natural land slide in the Navarro River, California with satisfactory results.

Overview of the Model

The numerical model presented here simulates the evolution of sediment pulses or disturbances in sediment input in mountain rivers. Grain size distribution of material coarser than 2 mm is used to characterize sediment; only bedload is considered in the model. Multiple lithologies are distinguished according to an abrasion coefficient. A standard backwater formulation is employed to solve for flow characteristics when the Froude number is not too high. If the Froude number is higher than a specified value (e.g., 0.75) the quasi-normal flow assumption is employed in place of the backwater calculation. Channel cross sections are simplified as rectangles of bankfull channel width, which is allowed to vary in the streamwise direction but not in time. The downstream boundary condition is a set bed elevation and normal flow assumption. The upstream boundary condition consists of specified daily water discharge, as well as a constructed sediment transport rating curve that satisfies an assumed set of quasi-equilibrium background conditions in the absence of sediment pulses. Tributaries are simplified to an input term that characterizes a downstream discharge increase that is proportional to the increase in drainage area. The background sediment input to the channel from tributaries and erosion of banks and terraces is constructed so that the overall profile at any given discharge is in a quasi-equilibrium state in the absence of pulses, i.e., both sediment supply and its grain size distribution are functions of local water discharge. The present model allows for only one sediment pulse. An arbitrary number of pulses can be accommodated, however, with only minor modification to the code. In addition to a sediment pulse, changes in sediment yield at the upstream end and along the river can be specified as continuous disturbances. The model is one-dimensional, and does not simulate such local features as point bars, pools, and riffles. This limitation is common among all the current one- or two-dimensional sediment transport models, possibly because sediment transport is linked only to local shear stress, and shear stress is calculated from depth-averaged shallow water equations. The channel bed is assumed to be composed entirely of gravel (the small fraction of sand and silt in the deposit is treated as pores), with no geological controls such as bedrock outcrops. Sand and finer material is treated as wash (throughput) load, and does not affect bed morphology in the model. Although natural channel response to sediment pulses is a complex, nonlinear, three-dimensional process, our simplified model provides a first-order approximation of channel response to sediment pulses, as demonstrated in the simulation of Navarro River landslide (Hansler 1999; Lisle et al. 2001; Sutherland et al. 2002).

Model Formulation and Solution Technique

Sediment transport models can be fully coupled (e.g., Rahuel et al. 1989; Holly and Rahuel 1990a,b) and decoupled (e.g., De Vries 1965; Ribberink 1987; Chen 1987; U.S. Army Corps of Engineers 1993; Cui et al. 1996). A fully coupled model acknowledges that sediment transport and flow occur simultaneously, and thus, their respective equations are coupled and should be solved simultaneously. A decoupled model realizes that the typical time scale for sediment transport and bed evolution is much longer than the typical time scale for water flow, and thus, at any given time, the flow can be approximated as in a steady state with respect to the bed profile at the moment without losing significant accuracy. This momentary steady flow assumption is usually termed as quasi-normal assumption, the validity of which can be found in a recent discussion paper (Cui et al. 2005b). The model presented in this paper adapts the treatment of a decoupled model, i.e., to alternate between the simulation of flow and bed evolution, and assume steady flow condition when flow is simulated.

Under the quasi-normal flow assumption, St. Venant shallow water equations can be simplified as the following backwater equation:

$$(1-\mathsf{F}^2)\frac{dH}{dx}=\mathsf{F}^2\frac{dB}{dx}+S_0-S_f-S_l \tag{1}$$

where F=the Froude number [$\mathsf{F}=Q_w/(g^{1/2}BH^{3/2})$ for a rectangular channel]; H=water depth; x=distance measured in the downstream direction; B=channel width; S_0=local bed slope; S_f=local friction slope; and S_l=a lateral friction contribution due to momentum exchange to the flow from tributaries:

$$S_0=-\frac{\partial\eta}{\partial x} \tag{2a}$$

$$S_f=\frac{u_*^2}{gH} \tag{2b}$$

$$S_l=\frac{2Q_wq_{wl}}{gB^2H^2} \tag{2c}$$

where Q_w=local water discharge; g=acceleration of gravity; η=bed elevation; u_*=shear velocity; and q_{wl}=lateral water discharge contribution per unit distance.

In Eqs. (2*a*) and (2*c*), S_0 scales with η_T/L and q_{wl} scales with Q_w/L, where η_T denotes the difference in bed elevation between the upstream and downstream ends of the study reach, and L denotes the length of the river. This leads to the estimate $S_l/S_0 \propto 2\mathsf{F}^2H/\eta_T$, or $S_l/S_0 \ll 1$. The term with dB/dx normally cannot be ignored. In this study, however, the channel width is assumed to be varying linearly along the channel, and $dB/dx \ll S_0$. Thus both the dB/dx and S_l terms are neglected in Eq. (1), further simplifying it to the standard backwater equation, which can be solved easily with a standard step method. The standard backwater solution, however, fails when the local Froude number approaches or exceeds unity. Cui et al. (1996) applied a time relaxation in order to treat the case of high Froude numbers. This technique was first tested in the present analysis and was found to give accurate results when the magnitude of the gravel pulse is high, although with a rather long computation time. When the magnitude of the gravel pulse becomes small, however, the numerical viscosity built into the model to dampen high frequency oscillations becomes dominant, resulting in unacceptable solutions. To avoid this problem with the numerical viscosity, the

technique of Cui et al. (1996) was abandoned in the present model and replaced with the technique used by the U.S. Army Corps of Engineers (1993), who applied the quasi-normal flow assumption whenever high Froude numbers are encountered. According to the quasi-normal flow assumption, Eq. (1) is further simplified as

$$S_0 = S_f \tag{3}$$

In the runs provided in this paper, the upper limit of the Froude number in applying the backwater formulation of Eq. (1) was set at 0.75, above which the formulation of Eq. (3) was used. It is useful to mention that the distance in calculating bed slope S_0 is the space increment used in the simulation, which is 250 m for the runs provided in this paper.

The quasi-normal flow assumption has been used in most numerical models for the transport of heterogeneous sediment, e.g., Diegaard (1980), Parker (1991a,b), and Cui and Parker (1997). By comparing results with Cui et al. (1996), Cui and Parker (1997) demonstrated that quasi-normal assumption adequately represented the full decoupled equations in case of flows with high Froude number. In the runs provided later in this paper, Froude number ranges from well below unity (e.g., in the backwater area upstream of the initial pulse) to much higher than unit at the steep downstream face of the initial sediment pulse.

Mass conservation of sediment is described in terms of the Exner relations for gravel mixtures, which can be found in continuous form in Parker (1991a,b), in discretized form in Parker (1990b) for the case of vanishing abrasion, and in Cui and Parker (1998) with the presence of basin subsidence and with uniform width. The Exner relation for total mass conservation of gravel used for the current model is

$$(1-\lambda_p)B\frac{\partial \eta}{\partial t} + \frac{\partial Q_G}{\partial x} + \sum_{j,k}\{\beta_k Q_G(p_{j,k}+F'_{j,k})\} + \frac{Q_G}{3\ln(2)}\sum_k \frac{\beta_k(p_{1,k}+F'_{1,k})}{\Delta\psi_1} = q_{Gl} \tag{4a}$$

and the Exner relation for mass conservation of gravel in the jth size range and the kth lithology takes the form

$$(1-\lambda_p)B\left(\frac{\partial(L_aF_{j,k})}{\partial t} + f_{I,j,k}\frac{\partial(\eta - L_a)}{\partial t}\right) + \frac{\partial(Q_G p_{j,k})}{\partial x} + \beta_k Q_G(p_{j,k}+F'_{j,k}) - \frac{\beta_k Q_G}{3\ln(2)}\left(\frac{p_{j+1,k}+F'_{j+1,k}}{\Delta\psi_{j+1}} - \frac{p_{j,k}+F'_{j,k}}{\Delta\psi_j}\right) = p_{l,j,k}q_{Gl} \tag{4b}$$

In the above relations the subscript j=jth grain size range and the subscript k=the kth lithology; λ_p=effective porosity of the deposit (gravel only); t=time; Q_G=volumetric gravel transport rate; L_a=active layer thickness; $f_{I,j,k}$,$p_{j,k}$=volume fractions of the jth grain size and the kth lithology in the material exchanged at the interface between the active layer and the substrate and in the bedload, respectively; β_k=abrasion coefficient (i.e., fraction of volume lost per unit distance transported) for the kth lithology; q_{Gl}=lateral volumetric input rate of gravel per unit distance (i.e., from erosion of terraces on the two banks and contribution from tributaries), which is a function of location and local discharge; $p_{l,j,k}$=fractions of the laterally contributed gravel in the jth grain size range and kth lithology; and ψ=logarithmic grain size defined as

$$\psi = -\phi = \log_2(D) \tag{5}$$

where ϕ=conventional base-2 logarithmic phi scale, and grain size D is in millimeters. The jth grain size range is described by the two bounding grain sizes $D_j(\psi_j)$ and $D_{j+1}(\psi_{j+1})$, from finer to coarser, and

$$\overline{\psi_j} = (\psi_j + \psi_{j+1})/2 \tag{6a}$$

$$\overline{D_j} = 2^{\overline{\psi_j}} = \sqrt{D_j D_{j+1}} \tag{6b}$$

$$\Delta\psi_j = \psi_{j+1} - \psi_j \tag{6c}$$

The fraction of material in the active layer in the jth size range and kth lithology is denoted as $F_{j,k}$. The parameter $F'_{j,k}$ in Eqs. (5a) and (5b) is an adjusted value of $F_{j,k}$ providing an estimate of relative surface area exposure of gravel of each grain size range and lithology at the surface, and is computed as (Parker 1991a,b)

$$F'_{j,k} = \frac{F_{j,k}/\sqrt{\overline{D_j}}}{\sum_{j,k}(F_{j,k}/\sqrt{\overline{D_j}})} \tag{7}$$

The active layer thickness L_a is taken as a constant in time at any location but can be different at different locations:

$$L_a = L_a(x) \tag{8}$$

The grain size fractions exchanged at the interface between the active layer and the substrate ($f_{I,j,k}$) are assumed to follow a relation derived from a set of large-scale experiments performed at St. Anthony Falls Laboratory (SAFL) and reported in Toro-Escobar et al. (1996);

$$f_{I,j,k} = \begin{cases} \chi p_{j,k} + (1-\chi)F_{j,k} & \text{bed aggradation} \\ p_{S,j,k} & \text{bed degradation} \end{cases} \tag{9}$$

where $p_{S,j,k}$ denotes the relevant fractions in the substrate immediately below the active layer and the empirical coefficient χ takes a value of 0.7. The option in Eq. (9) for aggradation is of the same form as a relation previously proposed by Hoey and Ferguson (1994). The fractions $F_{j,k}$, $f_{I,j,k}$, $F'_{j,k}$, $p_{j,k}$ and $p_{l,j,k}$ all refer to a grain size distribution that has been truncated so as to remove the sand, so that 100% of the material is coarser than 2 mm. It is useful to note that a value of 0.7 for χ was derived from laboratory sediment in which the surface layer was only on the order of grain diameters. It can be reasonably expected that a lower χ value will be more appropriate if a thicker active layer is used, and the numerical experiments of Hoey and Ferguson (1997) suggested that a different choice of χ value affects both the time scale of response and the degree to which aggradation is accompanied by surface coarsening or fining. The focus of this paper, however, is away from the examination of grain sorting, and it is expected that a different χ value will not likely alter the general pulse behavior.

A Keulegan-type resistance relation is used to quantify resistance at the bed in terms of shear velocity u_*:

$$\frac{Q_w}{BHu_*} = 2.5\ln\left(11\frac{H}{k_s}\right) \tag{10}$$

where roughness height k_s is assumed to take the value used by Cui et al. (1996),

$$k_s = 2D_{sg}2^{1.28\sigma_{s\psi}} \tag{11}$$

In the above relations D_{sg} denotes the geometric mean grain size of surface gravel and $\sigma_{s\psi}$ denotes the arithmetic standard devia-

tion of the grain size distribution of the surface material on the ψ scale. The roughness height calculated with Eq. (11) is a convenient approximation of that originally suggested by Parker (1990a,b).

The sediment transport equation used in the model is the surface-based bedload equation of Parker (1990a,b). Parker's bedload equation allows for the computation of the total bedload transport rate and the associated grain size distribution at a location with a specified local surface grain size distribution and the local shear velocity. No details of the surface-based bedload equation of Parker are presented here; readers are referred to the original publications (i.e., Parker 1990a,b) for details. Of importance here is the fact that the surface-based bedload equation of Parker (1990a,b) is restricted to grain sizes that are too coarse to participate substantially in suspension. The lower bound of 2 mm suggested in the original paper is also employed here. It is useful to note that it has been implicitly assumed that the sediment deposit is composed of mostly gravel, and the small amount of sand and silt is counted as pores in calculating the volume of a sediment deposit.

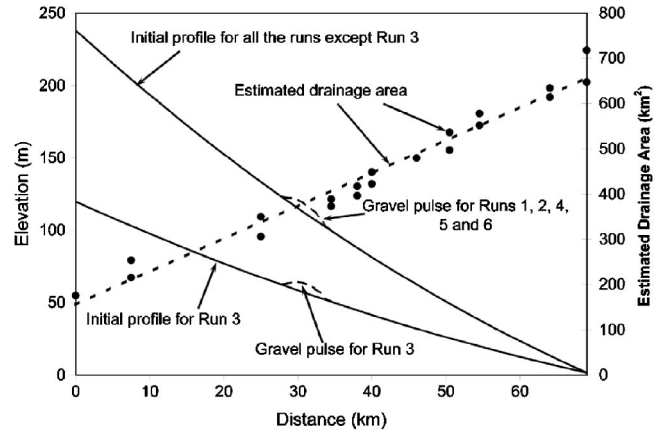

Fig. 1. Longitudinal profiles of the river to be simulated and the initial sediment pulses used in Runs 1–6; also shown are drainage area measurements (circles) measured from United States Geological Survey topographic maps, and the approximation (dashed line) used in the runs

Numerical Experiments: The Relative Importance of Major Parameters

Nine runs were conducted to examine the relative importance of various parameters to pulse evolution: Channel bed slope, water discharge, particle abrasion, and sediment supply. The variation of grain size distribution in pulse sediment has been examined both experimentally and numerically in Cui et al. (2003a,b), and thus is not discussed in this paper. Although the model was designed to handle a real-time hydrograph based on daily flows, the discharge used in each of the runs was set at a constant value. The reason for this is that with varied discharge the channel bed will experience periodic degradation and aggradation during and after flood events independently of any sediment pulse, making it difficult to identify whether morphologic variation results from the disturbance or varying discharge. Confining discharge to a constant value allowed for the examination of the effect of a single parameter on the evolution of sediment pulses.

The channel geometry used in the simulations is based on that of Redwood Creek near the city of Orick, California. The total length of the simulated river reach is 69 km, extending from Blue Lake to the mouth of the river near Orick. The width of the channel ranges from 40 m at the upstream end to 80 m at the downstream end. For simplicity, channel width at any point is interpolated linearly from the above widths. The longitudinal profiles for all the runs except Run 3 are taken to be the same as Redwood Creek, as shown in Fig. 1. The slope for Run 3 is lowered by a factor of 2 from that of the other runs, as shown in Fig. 1, to examine the effect of varied slope. The drainage area is assumed to increase linearly from 155 km^2 at the upstream end near Blue Lake to 660 km^2 at the downstream end near Orick, as shown in Fig. 1. The linear relation between drainage area and channel distance here is unique to Redwood Creek due to the long and narrow shape of the watershed. The assumed grain size distributions of the surface and subsurface gravel at the upstream and downstream ends are shown in Fig. 2. Grain size distributions at intervening cross sections are linearly interpolated from those at the upstream and downstream ends. The gravel pulses introduced in Runs 1–6 and Run 9 are arbitrarily set as parabolic shapes 6.5 m high and 6 km long centered at 31 km downstream of Blue Lake ($x=0$). The bulk volume of the gravel in each pulse is 1.4×10^6 m^3, containing approximately 2×10^6 t of gravel. The grain size distribution of the sediment that was introduced as initial pulses for the runs is also given in Fig. 2. No gravel pulses are introduced into Runs 7 and 8; instead the sediment supply is forced to deviate from its equilibrium value to serve as a disturbance. The gravel grain size distributions used for the runs are somewhat arbitrary and are only loosely based on the prototype river.

Initial conditions and results for each run are summarized in Table 1, and are detailed in the following:

Run 1: Base Run

Run 1 is the base run against which most other runs are compared. The discharge for Run 1 is set arbitrarily at 200 m^3/s at the

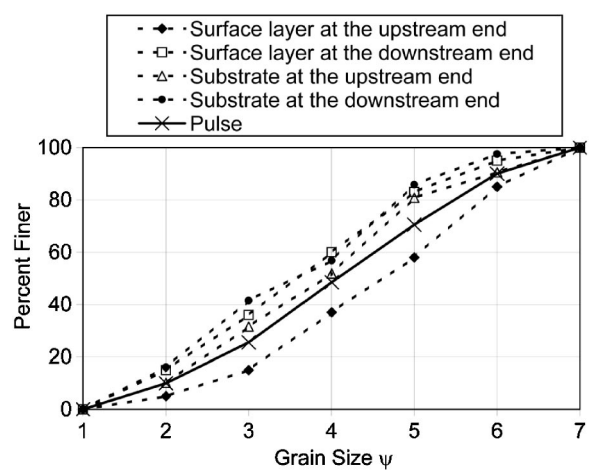

Fig. 2. Grain size distributions of the surface and subsurface at the upstream and downstream ends of the simulated reach, and grain size distribution of the introduced sediment pulse for the runs. The geometric mean (mm) and geometric standard deviation of those grain size distributions are (geometric mean, geometric standard deviation): upstream surface (23,3.84); upstream subsurface (14,4.07); downstream surface (12,3.88); downstream subsurface (11,3.68), and sediment pulse (17, 4.43).

Table 1. Summary of the Runs

	Difference from Run 1	Highlight of results
Run 1[a]		Sediment pulse disperses in time. Channel slope deviation from background equilibrium condition decreased to within 2% in 3 years.
Run 2	Discharge is half of that in Run 1.	Similar to Run 1 except that sediment pulse disperses more slowly. Sediment transport rate decreased by a factor of about 6.
Run 3	Slope is half of that in Run 1.	Similar to Run 1 except that sediment pulse disperses more slowly. Sediment transport rate decreased by approximately an order of magnitude.
Run 4	Abrasion coefficients for ambient and pulse sediment increased by an order of magnitude from Run 1.	The apex of the pulse translated upstream. Pulse sediment removed from the system much more rapidly than Run 1.
Run 5	Abrasion coefficient for pulse sediment increased by an order of magnitude from Run 1.	The apex of the pulse translated slightly upstream. Erosion is predicted downstream of the initial pulse location. Pulse sediment removed from the system much more rapidly than Run 1.
Run 6	Abrasion coefficient for ambient sediment increased by an order of magnitude from Run 1.	The amplitude of the pulse decreased in time, while the volume of the pulse first increased for approximately 10 years before it begin to decrease. Slight upstream translation of the apex is predicted. It takes a much longer time than Run 1 to remove the excess sediment from the system.
Run 7	No initial pulse is introduced. Instead sediment supply in the entire watershed is doubled for the first 10 years of simulation.	Bed aggradation occurred rapidly and continued throughout the period of the increased sediment loading. A large amount of excess sediment still exists in the system even 30 years after the cessation of the increased sediment loading.
Run 8	No initial pulse is introduced. Instead sediment supply is doubled in a short reach (32–35 km) for the first 10 years of simulation.	Regional increase in sediment loading resulted in aggradation of the entire watershed. The duration of the aggradation is much longer than that of the sediment overloading.
Run 9	Abrasion coefficients for ambient and pulse sediment set to zero.	Pulse evolution is slightly slower than in Run 1.

[a]Base run, a sediment pulse is introduced at the beginning of the run. Abrasion coefficients for ambient and pulse sediment are identical with a value of 0.01 km^{-1}.

downstream end near Orick, or about 0.31 $m^3/s/km^2$, which has an exceedance probability of approximately 0.017 based on the daily average discharge record between October 1, 1953 to September 30, 1993 at United States Geological Survey (USGS) station 11482500 Redwood Creek near Orick. The fixed discharge is applied to the river all the time and no "intermittency" is assumed in the simulation. With the assumption that discharge is proportional to local drainage area and the estimated drainage area shown in Fig. 1, the discharge decreases linearly in the upstream direction. The resulting discharge at the upstream end near Blue Lake is approximately 35 m^3/s. The volumetric abrasion coefficients of both the ambient and pulse gravel were set at 0.01 km^{-1}. Results for Run 1 are shown in Fig. 3(a) for incremental bed elevation (the amount of aggradation or degradation from the initial equilibrium longitudinal profile), Fig. 3(b) for normalized incremental bed slope, Fig. 3(c) for cumulative bedload transport, and Fig. 3(d) for surface mean grain size. The normalized incremental bed slope is defined as

$$\Delta S^*(x,t) = \frac{S_0(x,t) - S_e(x)}{S_e(x)} \tag{12}$$

in which ΔS^* = normalized incremental slope; S_e = equilibrium bed slope; and S_0 = channel bed slope as defined in Eq. (2*a*).

In Fig. 3(a), the pulse is seen to evolve by dispersion without any spatial translation of the pulse apex. As time advances, the pulse eventually evolves into a triangular deposit stretching over the entire reach, subsequently slowly degrading back to the initial equilibrium state.

Fig. 3(b) indicates that channel slope recovers toward the original equilibrium slope rather rapidly, even with the large amount of excess sediment still remaining in the system, as is evident from Fig. 3(a). Because one of the driving parameters of sediment transport is bed slope, the results in Fig. 3(b) indicate that the recovery rate of bed topography decreases as time advances.

The cumulative sediment transport curve shown in Fig. 3(c) indicates that the sediment transport rate increases in the downstream direction within the upper part of the reach because of lateral sediment input from the tributaries and the erosion of terraces on the two banks. Within the downstream part of the reach, however, the sediment transport rate decreases in the downstream direction because the lateral contribution from tributaries and erosion of terraces on the two banks is not enough to make up the amount of coarse sediment lost to abrasion.

It should be noted that the sediment transport rates predicted by the model do not correspond to the actual values in Redwood Creek because, as stated previously, a constant discharge is used for the simulation, and because the grain size distribution used for the simulation only loosely reflects the actual grain size distribution in the river.

Fig. 3(d) indicates that channel surface armored slightly within the first year of the introduction of the sediment pulse and then recovered rather quickly to the background condition.

Run 2: Test for Altered Discharge

Comparing the results for Runs 2 and 1 in Figs. 4(a) and 3(a) indicates that reducing discharge by a factor of 2 reduces the rate of pulse evolution. This reduction is due to the reduced bedload transport rate (by a factor of approximately 6), as is seen by comparing Fig. 4(b) with Fig. 3(c). The general pattern of sediment pulse evolution of Run 2, however, is similar to that of Run

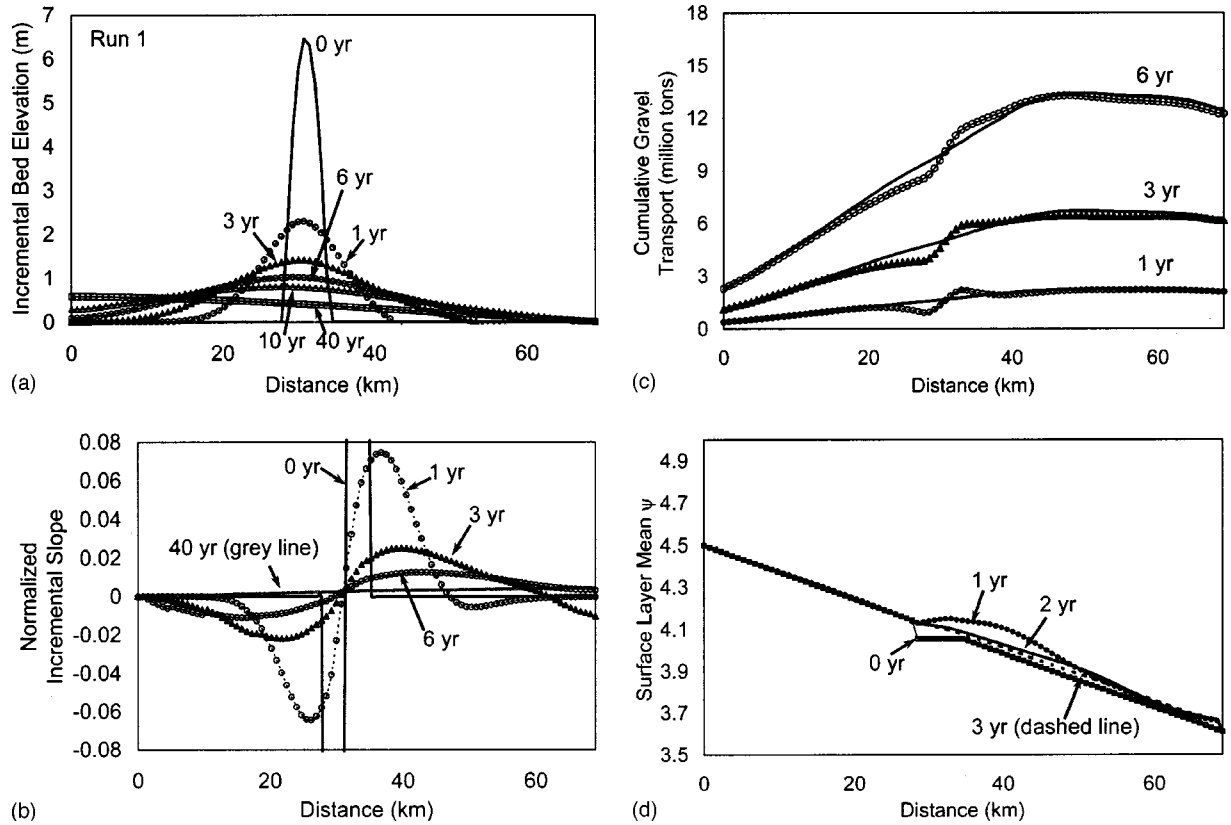

Fig. 3. Results of Run 1 with abrasion coefficients for both ambient and pulse sediment at 0.01 km^{-1}, and a discharge of 200 m^3/s at the downstream end of the study reach. (a) Incremental elevation; (b) normalized incremental bed slope; (c) cumulative gravel transport (solid lines without symbols are values under the background condition); and (d) surface layer mean grain size.

1. With the decreased shear stress compared to Run 1, the armoring effect associated with the introduction of the sediment pulse increased slightly [Figs. 4(c) and 3(d)]. In addition, the reduced shear stress also resulted in more fine sediment deposition in the backwater zone upstream of the sediment pulse. The other interesting observation in Run 2 is the minor but extensive degradation downstream of the initial pulse [Fig. 4(a)]. One possible explanation for the degradation is that the slightly stronger sorting in the pulse area due to a smaller discharge compared to Run 1 resulted in less coarser sediment supply further downstream, causing the minor but extensive degradation.

Run 3: Test for Altered Channel Slope

It is interesting to note that, with the reduced channel slope, the initial evolution of the pulse (at Year 1) is characterized by the erosion of the downstream face of the pulse and the development of a delta upstream of the pulse [Fig. 5(a)]. Fig. 5(a) shows that the delta is about to join the main pulse at the end of Year 1. Upstream delta development is caused by the backwater effect from the pulse, and is a common feature of the sediment pulse runs. In Run 1, for example, a delta joined with the main pulse during the early days of simulation and became indistinguishable from the main pulse by the end of Year 1. A very similar delta development was also observed in the SAFL sediment pulse experiment of Run 3 [see Cui et al. (2003a,b)] for details]. Indeed, a similar delta was observed in the Navarro River, Calif. due to the Floodgate slide (Hansler 1999; Lisle et al. 2001; Sutherland et al. 2002).

As in Run 2, the decreased shear stress resulted in a stronger armoring effect than in Run 1. It should be noted that the gravel transport rate in Run 3 is almost one order of magnitude smaller than that in Run 1 due to the reduced channel slope [Figs. 5(b) and 3(c)]. The reduced sediment transport rate in Run 3 results in slower evolution of the sediment pulse than in Run 1. Other than the reduced evolution speed for Run 3, the general pattern of pulse evolution of Run 3 is very similar to that of Run 1.

Run 4: Test for Higher Abrasion Coefficients of Both Ambient and Pulse Sediment

Results indicate that the sediment pulse evolved rather differently than in Run 1 due to the substantial increase in abrasion coefficients (Fig. 6). In particular, the apex of the sediment pulse is seen to move upstream. This phenomenon may appear strange but is easily explained in terms of less durable sediment in the river. Due to the large abrasion coefficient, a sediment particle can only travel a relatively short distance in the channel before it is completely consumed by abrasion. To demonstrate this point, we can perform an exercise by assuming a volumetric abrasion coefficient of 0.1 km^{-1} and applied the Sternberg's (1875) law [i.e., $V/V_0=\exp(-\beta x)$, $D/D_0=\exp(-\beta x/3)$, where V and D=volume and diameter of a sediment particle at distance x and V_0 and D_0 =volume and diameter of sediment particle at distance 0]. In this case a gravel particle will be reduced to about half of its original size and only 14% of its original volume within 20 km from the sediment source. With this in mind, it is not difficult to understand that the introduced sediment pulse will have an effect extending only a short distance in the downstream direction, so that the deposition rate downstream of the sediment pulse for Run 4 will

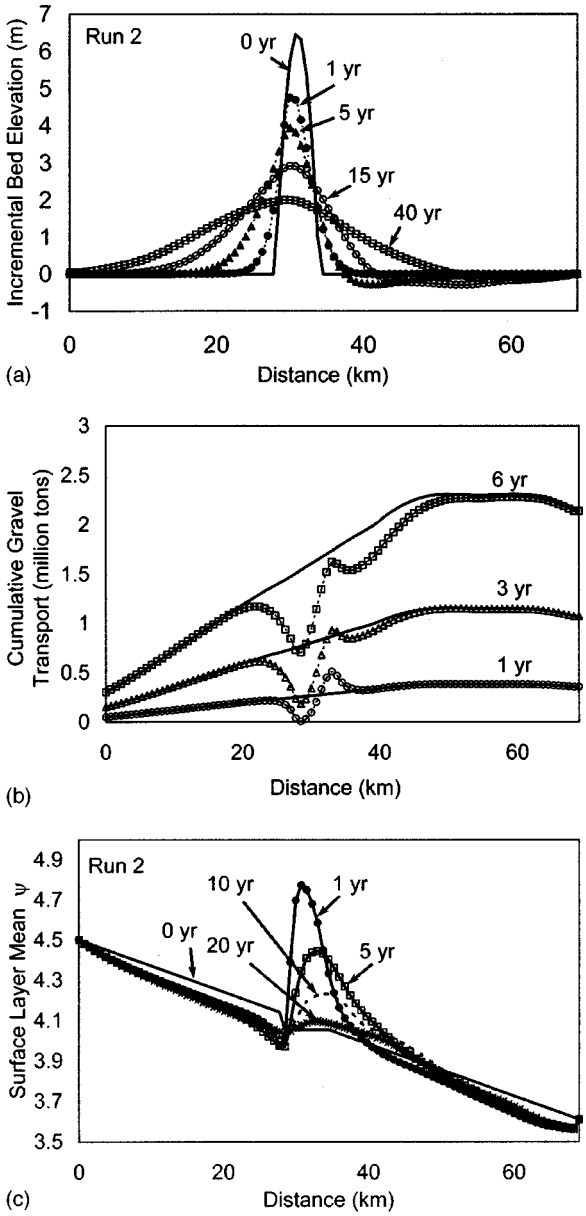

Fig. 4. Results of Run 2 with abrasion coefficients for both the ambient and pulse sediment at 0.01 km^{-1}, and a discharge of 100 m^3/s at the downstream end of the study reach. (a) Incremental elevation; (b) cumulative gravel transport (solid lines without symbols are values under the background condition); and (c) surface layer mean grain size.

be significantly less than that for Run 1. At the reach upstream of the pulse however, sediment deposition is caused by the backwater effect due to flow blockage from the sediment pulse, a phenomenon not directly related to abrasion. As a result, sediment continuously deposits upstream of the sediment pulse at a relatively high rate even with an increased abrasion coefficient. The combination of quick erosion of the downstream face of the sediment pulse, significantly reduced deposition farther downstream of the sediment pulse, and the continuous deposition in the backwater zone upstream of the sediment pulse results in the upstream migration of sediment pulse apex.

Fig. 6(b) indicates that surface grain size increased slightly throughout the studied reach and continued throughout the run duration. The reason for the slightly coarser surface layer is not

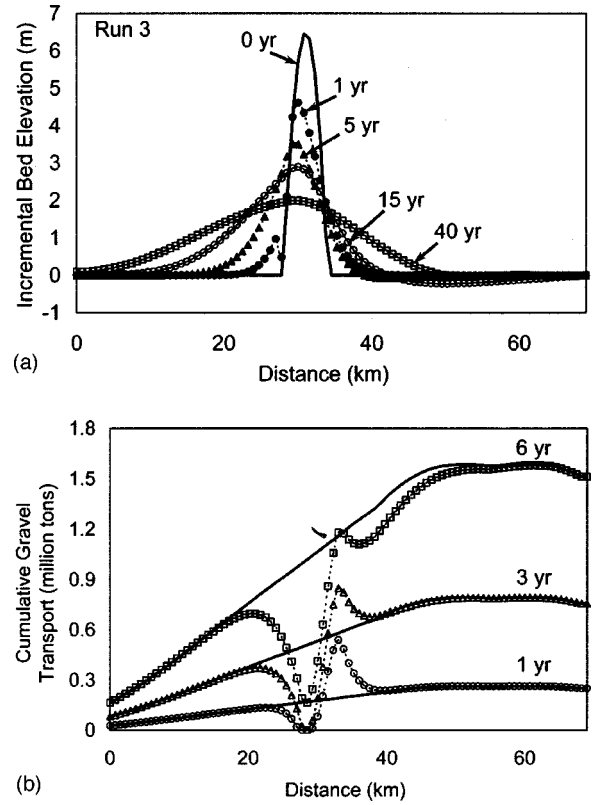

Fig. 5. Results of Run 3 with abrasion coefficients for both the ambient and pulse sediment at 0.01 km^{-1} and a discharge of 200 m^3/s at the downstream end of the study reach. Channel slope was reduced by a factor of 2 compared to the other runs as shown in Fig. 1. (a) Incremental elevation; and (b) cumulative gravel transport (solid lines without symbols are values under the background condition).

easily explainable. It has been speculated that the coarsening may be the result of (1) less abrasion compared to ambient condition in the reach upstream of the sediment pulses due to the reduced travel distances as a result of the backwater effect; (2) high abrasion coefficient that quickly grind gravel particles to sand and finer, which are not counted for in the model; and (3) cumulative rounding error in the model.

Run 5: Test for a Case with an Abrasion Coefficient of Pulse Sediment That is Higher than That of the Ambient Sediment

By introducing a less durable sediment pulse, model results indicate that the channel degrades in the reach downstream of the pulse and aggrades at the reach upstream, again a rather strange but easily explainable phenomenon (Fig. 7). Upon the introduction of the sediment pulse, sediment transport rates downstream of it are significantly increased over their ambient values due to increased channel slope on the downstream face of the pulse deposit. The increased sediment transport, however, is composed almost entirely of sediment from the pulse, which is subject to heavy abrasion. On the other hand, the more durable sediment that is supplied from upstream is trapped in the depositional zone upstream of the pulse due to the backwater created by it. With the significantly reduced transport of more durable ambient sediment downstream of the pulse, the less durable sediment eroded from the pulse decreases quickly both in transport rate and in grain size in the downstream direction, which can be seen in Fig. 7(b) by

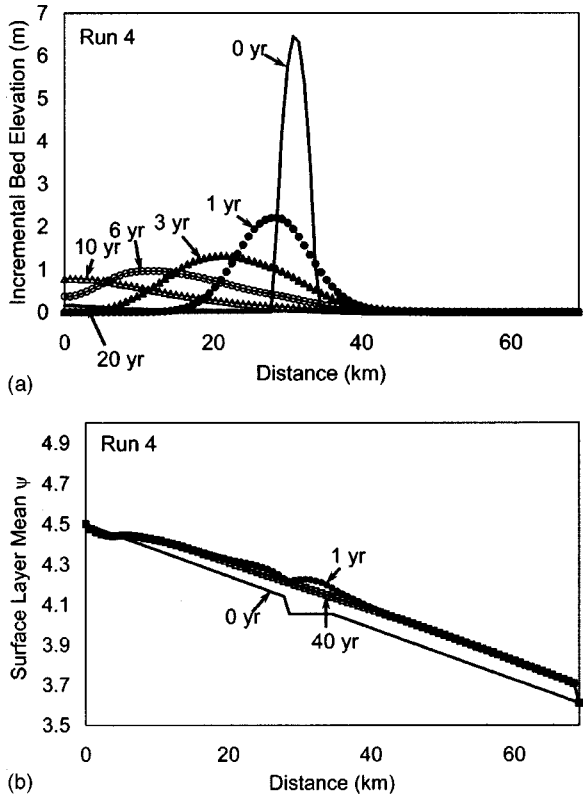

Fig. 6. Results for Run 4 with abrasion coefficients for both the ambient and pulse sediment at 0.1 km^{-1}, and a discharge of 200 m^3/s at the end of the study reach. (a) Incremental elevation and (b) surface layer mean grain size.

comparing Years 1 and 3 downstream of the station at 33 km, and in Fig. 7(c) for the slightly decreased surface mean grain size downstream of the pulse. As a result of the quick decrease in sediment transport rate and grain size, the channel bed downstream of the sediment pulse degrades until the more durable ambient sediment begins to pass through the pulse.

Run 6: Test for a Case with an Abrasion Coefficient of Pulse Sediment That is Lower than That of the Ambient Sediment

Results for Run 6 indicate that the excess sediment in the system increases in time for a considerable period with the introduction of a sediment pulse composed of more durable sediment than the ambient sediment (Fig. 8). This phenomenon can be easily explained by realizing that the less durable sediment is trapped upstream of the sediment pulse, and the bedload downstream of the pulse is replaced with the more durable pulse sediment. The exchange between the less durable ambient sediment and more durable pulse sediment results in a shorter distance of transport for the less durable ambient sediment. As a result, the loss of sediment due to abrasion becomes smaller compared with the equilibrium state. In addition, the transport of more durable sediment downstream of the pulse makes the characteristic grain size of the bedload slightly larger, which helps to reduce the amount of sediment transported out of the system. The increase in excess sediment volume retained in the river is the result of a combination of reduced abrasion and less sediment transport out of the system, whereas the supply is kept unchanged. The slightly upstream moving apex is most likely the result of the relatively quick

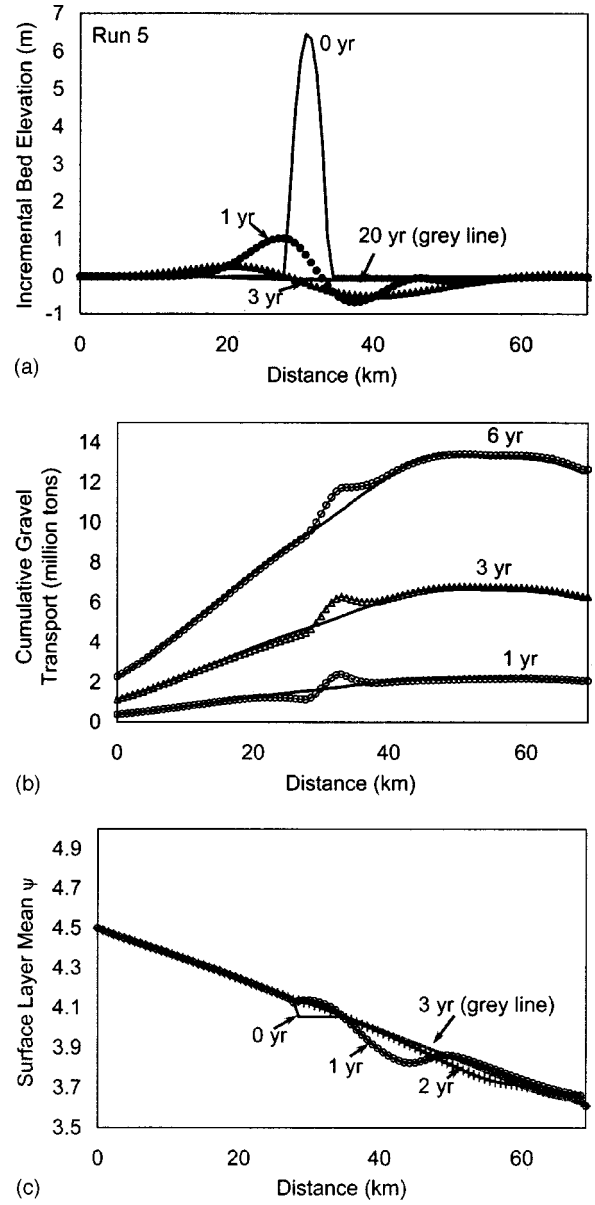

Fig. 7. Results of Run 5 with abrasion coefficients for ambient and pulse sediment at 0.01 and 0.1 km^{-1}, respectively, and a discharge of 200 m^3/s at the end of the study reach. (a) Incremental elevation; (b) cumulative gravel transport (solid lines without symbols are values under the background condition); and (c) surface layer mean grain size.

buildup of less durable sediment at the upstream face of the pulse coupled with the slow erosion of the more durable sediment at the downstream face.

Similar to Run 4, surface mean grain size increased slightly throughout the studied reach and remained high over the duration of the run.

Run 7: Test of Watershed-Scale Increase in Sediment Supply

Results for Run 7 indicate that doubling the sediment supply in the entire watershed results in large amount of aggradation in the entire study reach (Fig. 9). Although the increase in sediment supply is limited to the first 10 years, it takes a much longer time

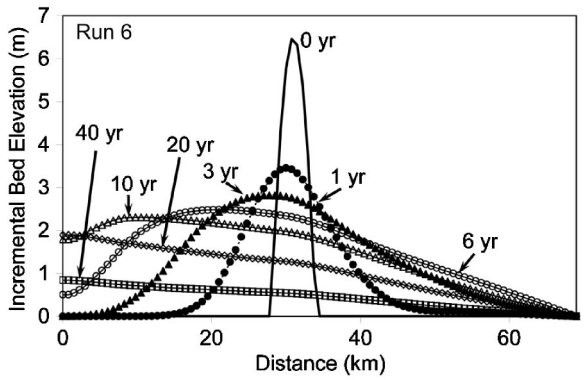

Fig. 8. Incremental elevation for Run 6 with abrasion coefficients for ambient and pulse sediment at 0.1 and 0.01 km^{-1}, respectively, and a discharge of 200 m^3/s at the end of the study reach

to transport the excess sediment out of the system. For example, even 30 years after the sediment supply has returned to its equilibrium value (40 years from the beginning of the simulation), there is still about 5.5 m of excess deposit at the upstream end of the reach. Similar to Run 1 presented in Fig. 3(c), the deviation of slope from its equilibrium value becomes smaller as the excessive sediment is transported out of the system. As a result, the transport of excess sediment out of the system becomes slower in time. It needs to be noted, however, that the large magnitude of aggradation in this run is an artificial effect due to the use of a constant discharge and a constant sediment supply rate associated with that discharge. This sediment supply is most likely much higher than a similar river system in the field because sediment supply and transport in natural rivers normally occur only for a very short period every year. As a result, it can be expected that the magnitude of aggradation in a natural river system will be much smaller than predicted in Run 7. Despite the expected smaller magnitude of aggradation in natural rivers, the conclusion that it will need a long period of time to work out the excess sediment remains the same.

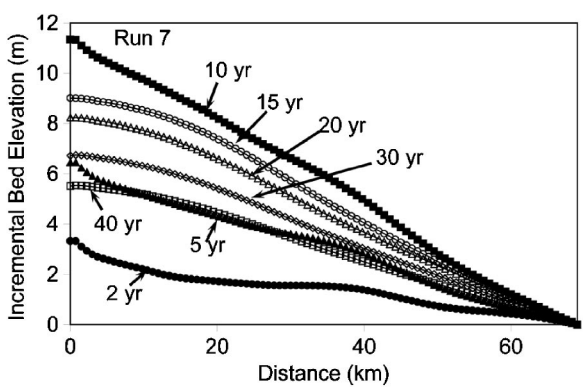

Fig. 9. Incremental elevation for Run 7 with abrasion coefficient at 0.01 km^{-1}, and a discharge of 200 m^3/s at the downstream end of the study reach. Sediment supply is doubled in the entire study reach for the first 10 years of simulation and then reduced to the equilibrium value.

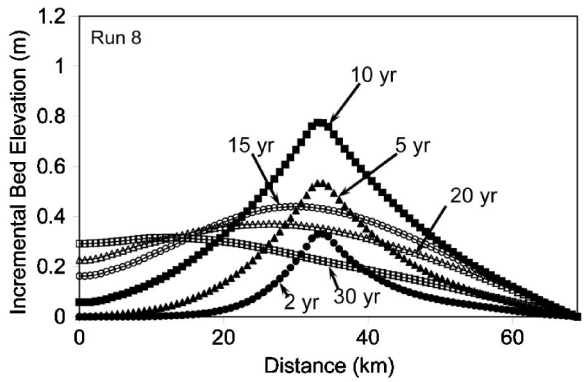

Fig. 10. Incremental elevation for Run 8 with abrasion coefficient at 0.01 km^{-1} and a discharge of 200 m^3/s at the downstream end of the study reach. Sediment supply was doubled at the reach between the stations at 32 and 35 km for the first 10 years and then reduced to the equilibrium value. Note the vertical scale is exaggerated by a factor of 10 from that of Fig. 9.

Run 8: Test of Local-Scale Increase in Sediment Supply

Results for Run 8 are presented in Fig. 10 for incremental elevation. It is interesting to note that a change in sediment supply within a very short reach for a specified period of time affects the entire basin for a much longer period of time. It needs to be cleared, however, that the magnitude of aggradation in this run is an order of magnitude smaller than that in Run 7. In addition, the magnitude of aggradation in a natural river will most likely be much smaller than predicted, as discussed earlier in Run 7.

Run 9: Test for Zero Abrasion

Results for Run 9 are very similar to that of Run 1, except that sediment pulse evolved slightly slowly. Details of the results for Run 9 are not presented here. The lack of major difference between Runs 9 and 1 indicates that the effect of abrasion becomes minimal for the evolution of the tested gravel pulse when abrasion coefficient is below 0.01 km^{-1}.

Conclusions

A numerical model for gravel mixtures is developed in order to simulate the evolution of (1) sediment pulses and (2) disturbances in the form of an increased sediment supply introduced to an equilibrium mountain river. The riverbed is assumed to be composed entirely of alluvial gravel without any geological controls such as bedrock outcrops or large boulder pavements. This assumption is usually not satisfied in natural mountain river systems, and thus, the model may need specific modifications when applied to a given natural river [e.g., Cui and Wilcox (2005)]. Although the model in its present form requires some modifications for site-specific applications, the version presented in this paper offers useful insight into the evolution of sediment pulses and disturbances due to increased sediment supply. The most important observations resulting from the numerical experiments presented above are as follows:

1. Sediment pulses in mountain rivers evolve predominantly by dispersion. This result confirms the findings of earlier field observations, flume experiments, and most numerical experi-

ments (e.g., Lisle et al. 1997, 2001; Hanlser 1999; Cui et al. 2003a,b). Translation of the apex is a secondary phenomenon that occur in certain situations (e.g., upstream translation in Run 4, in which both the ambient and pulse sediment are highly less durable).

2. Sediment pulses in rivers with higher bedload transport capacities (e.g., higher slope or discharge) evolve more quickly. This observation, intuitively obvious though it may be, has important implications. In many if not most mountain watersheds, the upper reaches of the river are usually steep, with geological controls such as bedrock outcrops and large boulder pavements, indicating a higher sediment transport capacity than sediment supply. The implication is that if a sediment pulse such as a landslide occurs in the upstream reaches of a river, the effect of that pulse may be minimal, or at least muted compared to an alluvial reach. This result is consistent to that of the numerical experiment by Hoey and Ferguson (1997) that systems with higher sediment transport capacity recover to equilibrium faster.
3. The abrasion of gravel is probably one of the most important mechanisms by which the excess sediment mass in a sediment pulse is transported out of the system. In the presence of abrasion, particles in the sediment pulses become finer in the downstream direction, easing their transport out of the system. Moreover, sediment that is abraded to sand and silt sizes will travel as washload in mountain rivers. This can greatly reduce the volume of the excess sediment transported as bedload, and thus accelerate the process for the river to return to its background equilibrium. In addition to the ability of abrasion to accelerate the evolution of sediment pulses, a difference in durability between ambient and pulse sediment, as reflected in their respective abrasion coefficients, may result in distinct and interesting differences in resulting channel morphology. In particular, in many cases it can be expected that the relatively freshly produced sediment in a landslide or debris flow is more easily abradable than gravel clasts which have been resident in the channel for a substantial amount of time. It is worth mentioning that the channel bed may be blanketed with sand if the amount of fine sediment produced from the pulse is extremely high, which is not simulated in the current model.
4. Excessive sediment input to a river system for a short period of time may result in excess sediment in the system for a long period of time before it can return to its equilibrium state. Excess sediment on a local scale may result in aggradation at a much larger spatial scale both upstream and downstream of the source of the disturbance.
5. Examinations of the effect of pulse grain size distribution are not presented in this paper. Limited examinations of the effect of pulse grain size distributions, however, have been conducted both experimentally and numerically and have been reported in Cui et al. (2003a,b). Results from both flume and numerical experiments in Cui et al. (2003a,b) indicate that coarser sediment pulses relative to ambient sediment evolve more slowly, whereas finer sediment pulses relative to ambient sediment exhibit more translation. Interested readers are referred to the original references for details.

We caution that the conclusions reached in this paper are based on a sediment transport model with many simplifications, including: constant discharge and constant sediment supply; rectangular channel cross section that ignores the effects of floodplains; the absence of grade controls; and the equilibrium pre-pulse longitudinal profile. It can be expected that the behavior of natural rivers is much more complicated than predicted in the runs. For example, experimental runs conducted with natural hydrographs have resulted in more variations of the evolution speed of sediment pulses in time; simulation of sediment transport following dam removal in a natural river with grade control indicated that sediment would deposit only in areas with low sediment transport capacities while bypass the reaches with high transport capacities (Cui and Wilcox, in press). It can be expected that more insights will be gained by further study of the full three-dimensional problem and associated processes not considered here.

Acknowledgments

This research was funded jointly by the U.S. Environmental Protection Agency and the U.S. National Science Foundation (EPA/R824779-01-0 and NSF/EAR-9524358). Resources supplied by the Minnesota Supercomputer Institute are gratefully acknowledged. The helpful comments from four anonymous reviewers have been incorporated into the manuscript.

Notation

The following symbols are used in this paper:

B = cannel width;
$\underline{D}_j$ = lower bound grain size of the jth size range;
$\overline{D}_j$ = geometric mean grain size of the jth range, $=\sqrt{D_j D_{j+1}}$;
D_{sg} = surface layer geometric mean grain size;
F = Froude number;
$F_{j,k}$ = volumetric fraction of the jth size range and kth lithology in surface layer;
$F'_{j,k}$ = aerial fraction exposed to the flow for the jth size range and kth lithology in surface layer;
$f_{I,j,k}$ = volumetric fraction of the jth size range and kth lithology in the sediment that is in exchange between bedload and channel bed;
g = acceleration of gravity;
H = water depth;
k_s = roughness height;
L = distance between the upstream and downstream ends;
L_a = surface layer (active layer) thickness;
$p_{j,k}$ = volumetric fraction of the jth size range and kth lithology in bedload;
$p_{l,j,k}$ = volumetric fraction of the jth size range and kth lithology in lateral gravel input;
$P_{s,j,k}$ = volumetric fraction of the jth size range and kth lithology in subsurface deposit;
Q_G = volumetric transport rate of gravel;
Q_w = water discharge;
q_{Gl} = lateral gravel contribution (due to tributaries), in volume per unit distance;
q_{wl} = lateral water discharge contribution (due to tributaries) per unit distance;
S_e = equilibrium channel bed slope;
S_f = friction slope;
S_l = lateral friction contribution from tributaries;
S_0 = channel bed slope;
t = time;
u_* = shear velocity;

x = downstream distance;
β_k = volumetric abrasion coefficient of gravel for the kth lithology;
ΔS^* = normalized incremental bed slope;
$\Delta\psi_j$ = $\psi_{j+1}-\psi_j$;
η = bed elevation;
η_T = difference in bed elevation between the upstream and downstream ends;
λ_p = porosity of the sediment deposit;
$\sigma_{s\psi}$ = arithmetic standard deviation of surface gravel;
ϕ = grain size ϕ scale $[=-\log_2(D)]$, where grain size D is in millimeters;
χ = empirical coefficient;
ψ_j = grain size ψ scale for the lower bound grain size of the jth size range, $=-\phi=\log_2(D_j)$, where grain size D_j is in millimeters; and
$\overline{\psi_j}$ = mean grain size ψ value for the jth size range, $=0.5(\psi_j+\psi_{j+1})$.

References

Benda, L., and Dunne, T. (1997). "Stochastic forcing of sediment routing and storage in channel networks." *Water Resour. Res.*, 33(12), 2865–2880.

Chen, Y. H. (1987). *Reservoir sedimentation model-RESSED*, User's Manual.

Cui, Y., and Parker, G. (1997). "A quasi-normal simulation of aggradation and downstream fining with shock fitting." *Int. J. Sediment Res.*, 12(2), 68–82.

Cui, Y., and Parker, G. (1998). "The arrested gravel-front: stable gravel-sand transitions in rivers. Part 2: General numerical solution." *J. Hydraul. Res.*, 36(2), 159–182.

Cui, Y., Parker, G., Braudrick, C., Dietrich, W. E., and Cluer, B. (2005a). "Dam removal express assessment models (DREAM), Part 1: Model development and validation." *J. Hydraul. Res.*, in press.

Cui, Y., Parker, G., Lisle, T. E., Gott, J., Hansler-Ball, M. E., Pizzuto, J. E., Allmendinger, N. E., and Reed, J. M. (2003a). "Sediment pulses in mountain rivers. Part I: Experiment." *Water Resour. Res.*, 39(9), 1239, doi: .

Cui, Y., Parker, G., Lisle, T. E., Pizzuto, J. E., and Dodd, A. M. (2005b). "More on the evolution of bed material waves in alluvial rivers." *Earth Surf. Processes Landforms*, 30, 107–114.

Cui, Y., Parker, G., and Paola, C. (1996). "Numerical simulation of aggradation and downstream fining." *J. Hydraul. Res.*, 32(2), 185–204.

Cui, Y., Parker, G., Pizzuto, J. E., and Lisle, T. E. (2003b). "Sediment pulses in mountain rivers. Part II: Comparison between experiments and numerical predictions." *Water Resour. Res.*, 39(9), 1240.

Cui, Y., and Wilcox, A. C. (2005). "Numerical modeling of sediment transport upon dam removal: Application to Marmot Dam in Sandy River, Oregon." *Sedimentation engineering, ASCE Manual 54*, Vol. 2, M. H. Garcia, ed., ASCE, Reston, Va.

De Vries, M. (1965). "Consideration about non-steady bed-load transport in open channels." *Proc., IAHR, 11th Congress*, 3.8.1–3.8.8.

Diegaard, R. (1980). "Longitudinal and transverse sorting of grain sizes in alluvial rivers." *Series Paper 26*, Institute of Hydrodynamics and Hydraulic Engineering, Technical Univ. of Denmark, Lyngby, Denmark.

Gilbert, G. K. (1917). "Hydraulic mining debris in the Sierra Nevada." *U.S. Geol. Surv. Prof. Pap.*, 105, 154.

Hansler, M. E. (1999). "Sediment wave evolution and analysis of a one-dimensional sediment routing model, Navarro River, Northwestern California." a thesis, The Faculty of Humboldt State Univ..

Hoey, T. B., and Ferguson, R. I. (1994). "Numerical simulation of downstream fining by selective transport in gravel bed rivers: Model development and illustration." *Water Resour. Res.*, 30, 2251–2260.

Hoey, T. B., and Ferguson, R. I. (1997). "Controls of strength and rate of downstream fining above a river base level." *Water Resour. Res.*, 33(11), 2601–2608.

Holly, F. M., and Rahuel, J. L. (1990a). "New numerical/physical framework for mobile-bed modeling. Part I: Numerical and physical principles." *J. Hydraul. Res.*, 28(4), 401–416.

Holly, F. M., and Rahuel, J. L. (1990b). "New numerical/physical framework for mobilebed modelling. Part II: Test applications." *J. Hydraul. Res.*, 28(5), 545–564.

James, L. A. (1991). "Incision and morphologic evolution of an alluvial channel recovering from hydraulic mining sediment." *Geol. Soc. Am. Bull.*, Vol. 103, 723–736.

Knighton, A. D. (1989). "River adjustments to changes in sediment load: the effects of tin mining on the Ringarooma River, Tasmania, 1875–1984." *Earth Surf. Processes Landforms*, 14, 333–359.

Lisle, T. E., Cui, Y., Parker, G., Pizzuto, J. E., and Dodd, A. M. (2001). "The dominance of dispersion in the evolution of bed material waves in gravel-bed rivers." *Earth Surf. Processes Landforms*, 26, 1409–1420.

Lisle, T. E., Pizzuto, J. E., Ikeda, H., Iseya, F., and Kodama, Y. (1997). "Evolution of a sediment wave in an experimental channel." *Water Resour. Res.*, 33(8), 1971–1981.

Parker, G. (1990a). "The ACRONYM series of PASCAL program for computing bedload transport in gravel rivers." *External Memorandum M-220*, Univ. of Minnesota, St. Anthony Falls Lab., Minn.

Parker, G. (1990b). "Surface-based bedload transport relation for gravel rivers." *J. Hydraul. Res.*, 28(4), 417–436.

Parker, G. (1991a). "Selective sorting and abrasion of river gravel. I: Theory." *J. Hydraul. Eng.*, 117(2), 131–149.

Parker, G. (1991b). "Selective sorting and abrasion of river gravel. II: Applications." *J. Hydraul. Eng.*, 117(2), 150–171.

Pickup, G., Higgins, R. J., and Grant, I. (1983). "Modelling sediment transport as a moving wave—The transfer and deposition of mining waste." *J. Hydrol.*, 60, 281–301.

Rahuel, J. L., Holly, F. M., Chollet, J. P., Belleudy, J. P., and Yang, G. (1989). "Modeling of riverbed evolution for bedload sediment mixtures." *J. Hydraul. Eng.*, 115(11), 1521–1542.

Ribberink, J. S. (1987). "Mathematical modeling of one-dimensional morphological changes in rivers with non-uniform sediment." *Rep. No. 87-2*, Delft University of Technology, Delft, The Netherlands.

Sternberg, H. (1875). "Untersuchungen über Langen-und Querprofil geschiebeführende Flüsse." *Zietschrift für Bauwesen*, 25, 483–506 (in German).

Sutherland, D. G., Hansler-Ball, M., Hilton, S. J., and Lisle, T. E. (2002). "Evolution of a landslide-induced sediment wave in the Navarro River, California." *GSA Bull.*, 114(8), 1036–1048.

Toro-Escobar, C. M., Parker, G., and Paola, C. (1996). "Transfer function for the desposition of poorly sorted gravel in response to streambed aggradation." *J. Hydraul. Res.*, 34(1), 35–54.

U.S. Army Corps of Engineers. (1993). "HEC–6, scour and deposition in rivers and reservoirs." Users Manual, ⟨http://www.hec.usace.army.mil/software/legacysoftware/hec6/hec6–documentaion.htm⟩ (accessed May 2005).

Weir, G. J. (1983). "One-dimensional bed wave movement in lowland rivers." *Water Resour. Res.*, 19(3), 627–631.